Abdominal Radiology (2019) 44:1816–1824
https://doi.org/10.1007/s00261-019-01931-6

Diagnostic value of MR-based texture analysis for the assessment of hepatic fibrosis in patients with nonalcoholic fatty liver disease (NAFLD)

Roberto Cannella[1,2] · Amir A. Borhani[1] · Mitchell Tublin[1] · Jaideep Behari[3] · Alessandro Furlan[1]

Published online: 20 February 2019

Abstract

Purpose To investigate the performance of MR-based texture analysis (TA) for the assessment of hepatic fibrosis in patients with nonalcoholic fatty liver disease (NAFLD).

Methods Fifty-four adult patients (33 females, 21 males, mean age 49.8 ± 13.5 years) with biopsy-proven NAFLD were enrolled and underwent MR imaging on a 1.5 T system. TA parameters were extracted on axial noncontrast 3D-GRE T1W images (slice thickness = 4.6 mm) using a commercially available research software (TexRAD). Receiver operating curves (ROC), areas under the ROC (AUROC) and 95% confidence intervals (CI) were calculated to assess the accuracy of each TA parameter for the diagnosis of significant ($F \geq 2$) and advanced fibrosis ($F \geq 3$). The correlation between TA and histopathological features of nonalcoholic steatohepatitis (NASH) was tested calculating the Spearman's rank correlation coefficient (ρ).

Results Thirty-seven (68%) subjects had significant fibrosis and 20 (37%) had advanced fibrosis. The TA parameters with the best performance were standard deviation (SD) and entropy, respectively, with AUROC 0.755 (95% CI 0.619–0.862, $p \leq 0.0002$) and 0.769 (95% CI 0.634–0.873, $p < 0.0001$) for significant fibrosis and AUROC 0.746 (95% CI 0.609–0.854, $p \leq 0.0004$) and 0.754 (95% CI 0.618–0.861, $p \leq 0.0002$) for advanced fibrosis. SD and entropy demonstrated a moderate correlation with the degree of fibrosis ($\rho = 0.457$ and 0.480; $p < 0.01$). No significant correlation was found between TA parameters and other histopathological features of NASH.

Conclusions Entropy and SD extracted on T1-weighted MR images have fair accuracy for the diagnosis of significant and advanced hepatic fibrosis in patients with NAFLD.

Keywords Texture analysis · Liver · Magnetic resonance · Hepatic fibrosis · Nonalcoholic fatty liver disease

Introduction

Nonalcoholic fatty liver disease (NAFLD) is one of the major causes of chronic liver disease in the Western world, affecting about 25% of the general population [1]. The progressive form of the disease, nonalcoholic steatohepatitis (NASH), can evolve to cirrhosis and lead to the development of hepatocellular carcinoma [2]. In this population, the risk of mortality is strongly associated with the grade of hepatic fibrosis [3–5]. Liver biopsy, the current reference standard for the assessment of hepatic fibrosis, is an invasive procedure with known complications (e.g., bleeding and pain) and limitations (e.g., inter-observer variability) making it unsuitable as a screening test [6, 7]. Thus, there is an unmet need for a noninvasive and accurate test for the quantification of hepatic fibrosis.

Texture analysis (TA) is an emerging imaging application that allows for quantification of the heterogeneity in an organ or focal lesion by analyzing the distribution and/or relationship of pixel gray levels of intensity within a region of interest (ROI) [8]. Although the role of TA for the evaluation of liver fibrosis has been previously explored on CT [9–11] and MR imaging [12–15], to the best of our knowledge, no study

✉ Alessandro Furlan
furlana@upmc.edu

1 Department of Radiology, University of Pittsburgh School of Medicine, 200 Lothrop Street, Pittsburgh, PA 15213, USA

2 Section of Radiology - Di.Bi.Med, University Hospital "Paolo Giaccone", Via del Vespro 129, 90127 Palermo, Italy

3 Department of Medicine, Division of Gastroenterology, Hepatology and Nutrition, University of Pittsburgh School of Medicine, Pittsburgh, PA 15213, USA

has focused on the value of MR-based TA in staging hepatic fibrosis in a NAFLD population. We hypothesize that the progressive accumulation of hepatic fibrosis is associated with significant and quantifiable changes in the distribution and heterogeneity of signal intensity, and therefore of TA parameters, within the liver parenchyma.

The aim or our study was to explore the performance of MR-based TA for the diagnosis of hepatic fibrosis in patients with NAFLD.

Materials and methods

The institutional review board approved this HIPAA-compliant study. This is a retrospective analysis of MR images obtained prospectively as part of a study aimed at evaluating the role of ultrasound- and MR-based elastography in the quantification of liver fibrosis in NAFLD. All subjects provided written informed consent before enrolling in the study.

Population

Between October 2015 and October 2017, 56 adult patients with NAFLD and no other cause of hepatic steatosis (i.e., history of alcohol abuse) or coexisting etiologies of chronic liver disease were included. Two patients were excluded because could not complete the MR examination for a suspected metallic foreign body ($n=1$) or claustrophobia ($n=1$). The final population consisted of 54 subjects. There were 21 (39%) men and 33 (61%) women with a mean age 49.8 ± 13.5 years (range 19–69 years) (Table 1). All enrolled patients had previously completed a clinically indicated liver biopsy within 1 year of enrollment that confirmed the diagnosis of NAFLD.

Table 1 Baseline characteristics of the study population

	Overall (54 patients)	Significant fibrosis (37 patients)	Advanced fibrosis (20 patients)
Gender			
Male	21 (39)	14 (38)	4 (20)
Female	33 (61)	23 (62)	16 (80)
Age (years)	49.8 ± 13.5	52.7 ± 11.7	55.5 ± 10.2
BMI (kg/m^2)	35.0 ± 7.4	35.5 ± 7.2	35.7 ± 7.1
Fibrosis score			
F0	1 (2)	0 (0)	0 (0)
F1	16 (30)	0 (0)	0 (0)
F2	17 (31)	17 (46)	0 (0)
F3	12 (22)	12 (32)	12 (60)
F4	8 (15)	8 (22)	8 (40)
NAS	5 ± 1.2	5 ± 1.1	5 ± 1.0
Steatosis grade			
0 (< 5%)	0 (0)	0 (0)	0 (0)
1 (5–33%)	13 (24)	5 (14)	0 (0)
2 (> 33%–66%)	23 (43)	16 (43)	10 (50)
3 (> 66%)	18 (33)	16 (43)	10 (50)
Inflammation			
0 (no foci)	1 (2)	0 (0)	0 (0)
1 (< 2 foci per 200×)	41 (76)	27 (73)	14 (70)
2 (2-4 foci per 200×)	12 (22)	10 (27)	6 (30)
3 (< 4 foci per 200×)	0	0 (0)	0 (0)
Ballooning			
0 (none)	1 (2)	0 (0)	0 (0)
1 (few balloon cells)	33 (61)	20 (54)	10 (50)
2 (many cells)	20 (37)	17 (46)	10 (50)

Continuous variables are expressed as mean and standard deviation, categorical variables are expressed as numbers and percentages

BMI body mass index, *NAS* NAFLD activity score

Reference standard

The histological evaluation of liver specimens obtained with percutaneous or intraoperative biopsy (16 or 18 G needles) was considered the reference standard for the study. Hepatic fibrosis was graded as follows: F0, absence of fibrosis; F1, perisinusoidal or periportal; F2, perisinusoidal and portal/periportal; F3, septal or bridging fibrosis; and F4, cirrhosis. Grades F2–F4 were categorized as significant fibrosis, while grades F3–F4 were categorized as advanced fibrosis. NAFLD activity score (NAS), grade of steatosis (0–3), lobular inflammation (0–3) and hepatocytes ballooning (0–2) [16] were also recorded from pathological reports according to NASH Clinical Research Network scoring system. NAS is the unweighted sum of the scores of steatosis, lobular inflammation and ballooning and ranges from 0 to 8 [16].

MR imaging technique

All patients were scanned on a 1.5 T MR (Optima MR450w or Signa HDxt; General Electric, Healthcare, Milwaukee, WI, USA) using an abbreviated imaging protocol including MR elastography (MR touch), coronal T2-weighted single shot fast spin echo (SSFSE), and axial T1-weighted three-dimensional (3D) gradient-recalled echo (GRE) imaging (Liver Acquisition with Volume Acceleration, LAVA) conducted without the use of IV contrast. The axial T1-weighted 3D GRE imaging was acquired with the following parameters: slice thickness, 4.6 mm; TR, 6.26 ms; TE, 3.126 ms; FA, 12°; FOV, 360–500 mm; matrix, 288 × 192.

Texture analysis

The TA parameters were extracted from the axial T1-weighed 3D GRE images utilizing a commercially available research software (TexRAD version 3.9, Feedback Plc, Cambridge, UK). The analysis was conducted by a single investigator (R.C., research fellow in abdominal imaging with 4 years of experience in cross-sectional imaging and 6 months of experience in TA) blinded to the clinical evaluation and to the pathological grading of fibrosis. A 3 cm^2 circular ROI was placed in the anterior segment of the right hepatic lobe on an image obtained at the level of the porta hepatis avoiding hepatic vessels, fissure and artifacts. A similar methodology was used in prior studies investigating the role of TA in liver fibrosis [13, 14, 17]. Using first-order statistical approach, five histogram-based parameters were automatically extracted including: mean, standard deviation (SD), mean of the positive pixel (mpp), skewness, and kurtosis. Entropy of pixels within the ROI was also automatically calculated based on the formula described in the previous works [18]. All the TA features included in this study were extracted from unfiltered images. The mean represents the average pixel grey-level intensities; SD represents the width of the histogram with dispersion from the mean; the entropy is quantified mathematically and measures the image inhomogeneity and irregularity [18, 19]; mpp is defined as the average of the positive pixel values; skewness is an indicator of the asymmetry of the histogram; kurtosis represents the peakedness/flatness of the histogram [20, 21].

Statistical analysis

Data were summarized as frequencies and percentages for categorical variables and as mean, range, and standard deviation (SD) for continuous variables. Receiver operating characteristics (ROC) and areas under the ROC curve (AUROC; with 95% confidence intervals) were calculated to assess the diagnostic performance of each TA parameter for the diagnosis of significant and advanced fibrosis. Optimal cutoff values were also calculated along with their corresponding sensitivity and specificity. The correlation between TA parameters, fibrosis and histopathological features of NASH (i.e., NAS, steatosis, inflammation and ballooning) was tested calculating the Spearman's rank correlation coefficient (Spearman's ρ).

Statistical significance level was set at $p < 0.05$. Statistical analysis was conducted using SPSS software (version 18.0; SPSS, Chicago, Ill) and MedCalc for Windows (version 17.1, MedCalc Software, Ostend, Belgium).

Results

The characteristics of the final population are summarized in Table 1. The distribution of fibrosis stage in the 54 subjects was as follows: F0, $n = 1$ (2%); F1, n = 16 (30%); F2, $n = 17$ (31%); F3, $n = 12$ (22%) and F4, $n = 8$ (15%). Thirty-seven (14 males and 23 females, mean age 52.7 ± 11.7 years) subjects had significant fibrosis, while 20 (4 males and 16 females, mean age 55.5 ± 10.2 years) subjects had advanced fibrosis.

The AUROC values of each TA parameter for the diagnosis of significant and advanced fibrosis are reported in Tables 2 and 3. SD and entropy showed the best performance in predicting the presence of significant and advanced fibrosis (Figs. 1, 2). For the diagnosis of significant fibrosis, SD showed an AUROC of 0.755 (95% CI 0.619–0.862) while entropy had an AUROC of 0.769 (95% CI 0.634–0.873) (Fig. 3). For the diagnosis of advanced fibrosis, SD showed an AUROC of 0.746 (95% CI 0.609–0.854) while entropy had an AUROC of 0.754 (95% CI 0.618–0.861) (Fig. 4). A SD value > 16.3 had a sensitivity of 49% and a specificity of 100% for the diagnosis of significant fibrosis and a sensitivity of 65% and a specificity of 85% for the diagnosis of advanced fibrosis. An entropy value > 4.1 had a sensitivity of

Table 2 Area under the receiver operating characteristic curve (AUROC), 95% confidence interval (95% CI), sensitivity (Se) and specificity (Sp) of the texture analysis parameters for the diagnosis of significant fibrosis (F2–F4)

Texture parameter	AUROC	95% CI	*p*	Cutoff	Se (%)	Sp (%)
Mean	0.639	0.497–0.765	0.0798	> 218.2	67	65
SD	0.755	0.619–0.862	0.0002	> 16.3	49	100
Entropy	0.769	0.634–0.873	< 0.0001	> 4.1	48	100
Mpp	0.639	0.497–0.765	0.0798	> 218.2	68	65
Skewness	0.650	0.508–0.775	0.0823	> − 0.0823	84	47
Kurtosis	0.463	0.396–0.674	0.7020	< − 0.06	81	47

SD standard deviation, *mpp* mean of the positive pixel

Table 3 Area under the receiver operating characteristic curve (AUROC), 95% confidence interval (95% CI), sensitivity (Se) and specificity (Sp) of the texture analysis parameters for the diagnosis of advanced fibrosis (F3–F4)

Texture parameter	AUROC	95% CI	*p*	Cutoff	Se (%)	Sp (%)
Mean	0.663	0.522–0.786	0.0367	> 238.6	70	65
SD	0.746	0.609–0.854	0.0004	> 16.3	65	85
Entropy	0.754	0.618–0.861	0.0002	> 4.1	65	85
Mpp	0.663	0.522–0.786	0.0367	> 238.6	70	65
Skewness	0.563	0.421–0.698	0.4330	> 0.07	70	53
Kurtosis	0.459	0.400–0.678	0.608	< 0.19	70	47

SD standard deviation, *mpp* mean of the positive pixel

48% and a specificity of 100% for the diagnosis of significant fibrosis and a sensitivity of 65% and a specificity of 85% for the diagnosis of advanced fibrosis (Fig. 5).

SD and entropy demonstrated a moderate and statistically significant ($p < 0.01$) correlation with the degree of fibrosis (SD $\rho = 0.457$; entropy $\rho = 0.480$). The correlation between TA parameters and other histopathological features of NASH, including NAS, steatosis, inflammation and ballooning was weak or very weak and not statistically significant (Table 4).

Discussion

In this prospectively-enrolled NAFLD population, the MR-based TA parameters, SD and entropy were positively correlated with the degree of liver fibrosis ($p < 0.01$) and showed fair accuracy for the diagnosis of significant (AUROC of 0.755 and 0.769, respectively) and advanced fibrosis (AUROC of 0.746 and 0.754, respectively). Higher SD values reflect a wider histogram of pixel intensities with larger dispersion of values from the mean [20]. On the other hand, higher entropy reflects more irregular and disorganized distribution of pixels with different intensities [18]. The architectural changes in the hepatic parenchyma and the deposition of collagen fibers that occur during fibrosis accumulation may explain the changes in the parenchymal heterogeneity.

To the best of our knowledge, ours is the first study investigating the use of TA parameters for the assessment of hepatic fibrosis in a well characterized NAFLD population. Recently, Naganawa et al. [22] using a NAFLD population and noncontrast CT imaging showed that mean, skewness and kurtosis were helpful in predicting the risk of NASH, defined as NAS ≥ 3. Interestingly, in our study none of the other histologic parameters of NASH (i.e., steatosis, inflammation and ballooning) showed a significant correlation with TA parameters suggesting that, when evaluated on MRI, these factors may not represent confounders in the assessment of hepatic fibrosis. Other studies have explored MR-based TA for assessment of hepatic fibrosis in cohorts of subjects with different etiologies of liver disease. House et al. [12] reported an AUROC of 0.51–0.74 for classifying advanced fibrosis using 14 Haralick TA parameters extracted on T2-weighted MR images. The population in that study consisted of 49 patients with chronic liver disease, of which 7 (14%) had NAFLD. Wu et al. [13] applied TA on T2-weighted and pre- and post-contrast T1-weighted imaging ($n = 279$ TA parameters) in 125 patients with chronic hepatitis C reporting misclassification rates for fibrosis stage and necroinflammatory activity grade as high as 35.77% and 34.15%, respectively. Zhang et al. [17] reported a higher performance of TA parameters extracted on MR images compared to those extracted on CT images for staging hepatic fibrosis. Among the TA parameters included in that study, mean and entropy were the most discriminative features regardless of the imaging method used.

In NAFLD, hepatic fibrosis represents an independent predictor of liver-related mortality [3–5, 23]. The need for a noninvasive alternative to liver biopsy has led to the extensive investigation of imaging methods for the quantification of liver fibrosis, most notably ultrasound- and

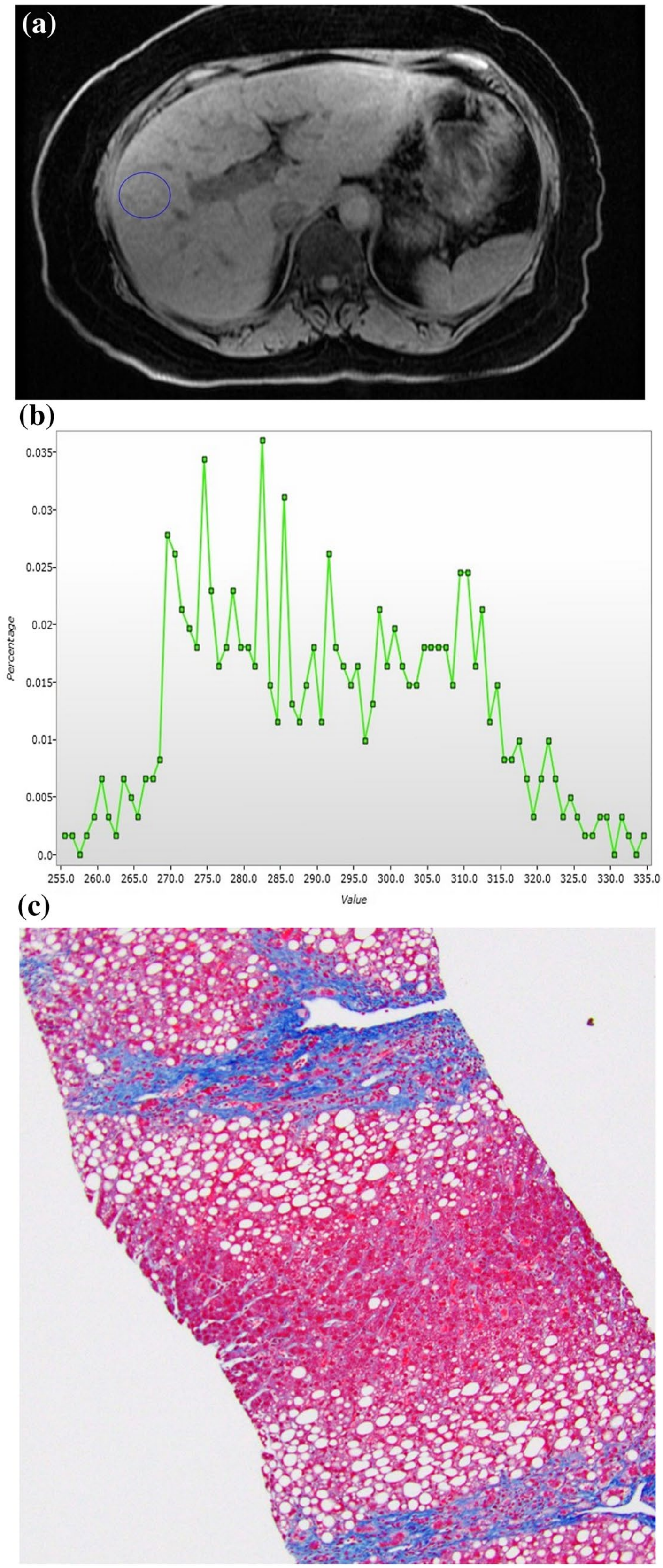

Fig. 1 58-year-old woman with biopsy-proven NAFLD. Texture analysis was performed by drawing a circular region of interest in the right hepatic lobe on axial T1-weighted image (**a**) and the corresponding unfiltered histogram of the texture parameters was extracted (**b**). Texture analysis demonstrated a SD of 16.9 and entropy of 4.12, both above the cutoff for the diagnosis of advanced fibrosis. Histopathologic analysis (H&E staining) of liver biopsy (**c**) showed F3 (bridging fibrosis), grade 3 steatosis, grade 2 inflammation and grade 1 ballooning (NAS = 6)

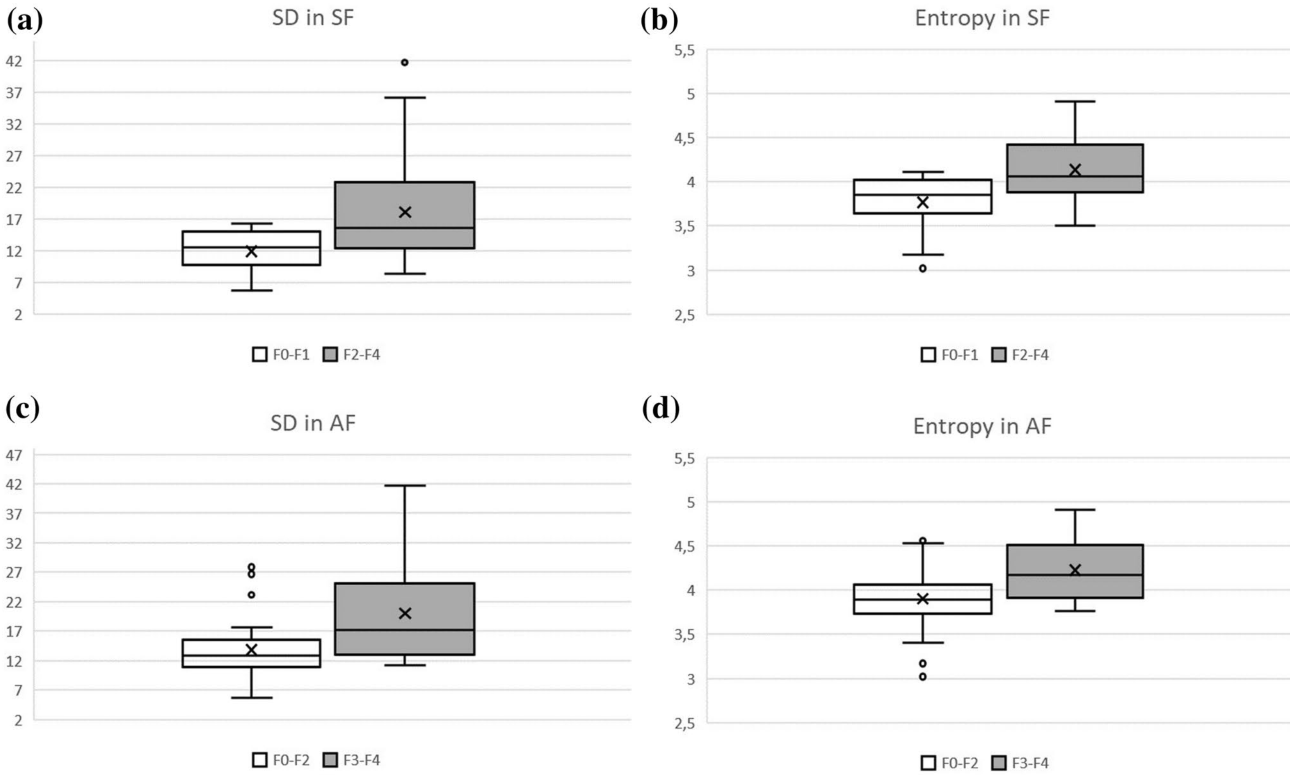

Fig. 2 Plot box illustrating the distribution of standard deviation (SD) and entropy in patients with different degrees of fibrosis. **a**, **b** SF: significant fibrosis (F2–F4); **c**, **d** AF: advanced fibrosis (F3–F4)

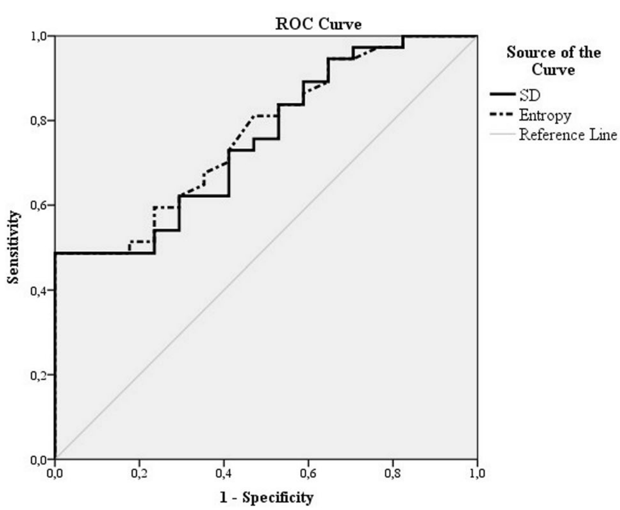

Fig. 3 Receiver operating characteristic (ROC) curve of standard deviation (SD) and entropy for the diagnosis of significant fibrosis (F2–F4)

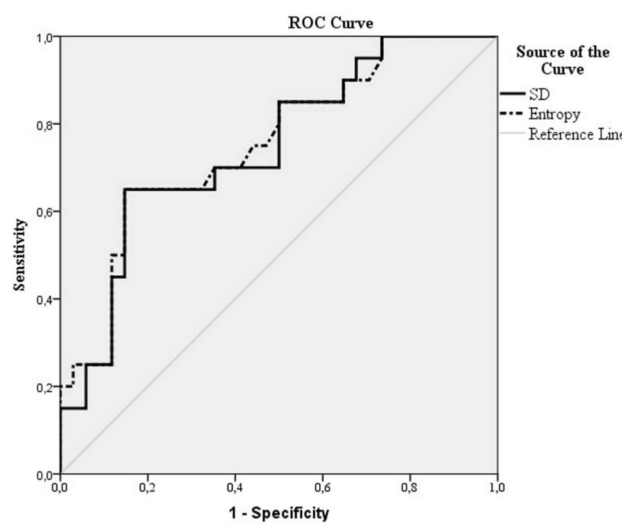

Fig. 4 Receiver operating characteristic curve (ROC) of standard deviation (SD) and entropy for the diagnosis of advanced fibrosis (F3–F4)

MR-based elastography [24] and diffusion weighted imaging [25]. Although the elastography techniques have shown good accuracy for staging hepatic fibrosis in patients with NAFLD [26], a prospective acquisition with dedicated hardware or sequences is required. Moreover, the use of liver stiffness measurement for the noninvasive assessment of fibrosis may be affected by confounders such as acute inflammation, biliary obstruction and hepatic

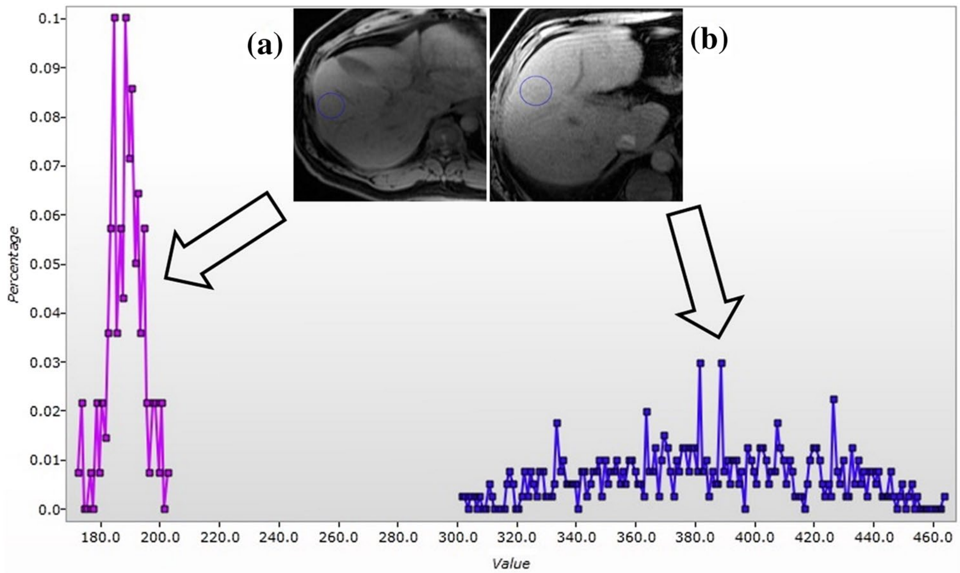

Fig. 5 Comparison of histograms of pixel intensities distribution and TA parameters in non-advanced and advanced fibrosis. **a** Histogram of pixel intensities distribution obtained from a circular ROI placed on an axial T1-weighted MR image of a 57-year-old man with F1 fibrosis. Texture analysis demonstrated a SD of 5.74 and entropy of 3.02. **b** Histogram of pixel intensities distribution obtained from a circular ROI placed on an axial T1-weighted MR image of a 35-year-old man with F4 fibrosis. The histogram in **b** shows a more heterogeneous distribution of pixel intensities than in **a** resulting in a wider and flatter shape. Texture analysis in **b** demonstrated a SD of 36.9 and entropy of 4.75

Table 4 Correlation between texture analysis parameters, fibrosis and histopathological markers of non-alcoholic steatohepatitis

Texture parameter	Fibrosis	NAS	Steatosis	Inflammation	Ballooning
Mean	0.255	0.130	0.036	0.262	−0.014
SD	0.457*	0.136	0.019	0.170	0.124
Entropy	0.480*	0.140	0.029	0.180	0.118
Mpp	0.255	0.130	0.036	0.262	−0.014
Skewness	0.135	0.046	0.048	0.078	−0.029
Kurtosis	−0.068	0.172	0.251	−0.225	0.209

Numbers represent the Spearman's rank correlation coefficient (ρ)

SD standard deviation, *mpp* mean of the positive pixel; NAS: NAFLD activity score

*Statistically significant

venous congestion [27]. Compared to other techniques, TA can be applied both prospectively and retrospectively on routinely acquired cross-sectional imaging without the need for dedicated hardware. The main current limitations of TA are the lack of a formally standardized methodology and its vulnerability to image acquisition and reconstruction parameters [28]. The availability of multiple research and commercial software solutions based on different analysis and statistical methods makes the comparison among different studies challenging and may eventually limit the use of TA in clinical practice [21, 24, 29, 30]. In our study, we applied TA on a set of images acquired prospectively with constant scanning parameters, thus mitigating some of the variability related to imaging technique [31, 32].

We recognize the following limitations of our study. The study population was small ($n=54$) and enrolled in a tertiary care clinic at a single center, and our results need to be confirmed in larger multicenter studies. Because of the small number of subjects enrolled with liver fibrosis stage F0 ($n=1$) and F4 ($n=8$), an analysis of the diagnostic accuracy of TA parameters for detection of any degree of fibrosis versus no fibrosis and for the detection of cirrhosis was not conducted. The choice of dichotomizing the population using F2 and F3 as cutoff fibrosis stages was based on clinical needs, since those values commonly dictate management in patients with NAFLD. The TA parameters were extracted using a single circular ROI with fixed surface area, following the methodology used on prior investigations [13, 14, 17] to guarantee a reproducible approach [33]. Although a three-dimensional or multi-slice approach may capture more tissue heterogeneity, this method is time-consuming, and its clinical advantage remains unclear [34].

In conclusion, entropy and SD extracted on T1-weighted MR images have fair accuracy for the diagnosis of significant and advanced hepatic fibrosis in patients with NAFLD. Further research is warranted to explore TA as a diagnostic tool in epidemiological studies and clinical care for staging NAFLD-associated liver fibrosis.

Funding The study is a retrospective analysis of MR images acquired as part of a prospective study conducted with financial and equipment support from General Electric. The sponsor had no involvement in the collection, analysis and interpretation of the data, in the writing of the report and in the decision to submit the article for publication.

Compliance with ethical standards

Conflict of interest The authors declare that they have no conflict of interests.

Disclosure Alessandro Furlan: research grant from General Electric; consultant for Elsevier/Amirsys. Amir A. Borhani: consultant for Guebert; consultant for Elsevier/Amirsys.

Ethical approval All procedures performed in studies involving human participants were in accordance with the ethical standards of the institutional and/or national research committee and with the 1964 Helsinki Declaration and its later amendments or comparable ethical standards.

Informed consent Informed consent was obtained from all individual participants included in the study.

References

1. Younossi ZM, Koenig AB, Abdelatif D, Fazel Y, Henry L, Wymer M (2016) Global epidemiology of nonalcoholic fatty liver disease-Meta-analytic assessment of prevalence, incidence, and outcomes. Hepatology 64:73–84.
2. Younossi ZM, Otgonsuren M, Henry L, Venkatesan C, Mishra A, Erario M, Hunt S (2015) Association of nonalcoholic fatty liver disease (NAFLD) with hepatocellular carcinoma (HCC) in the United States from 2004 to 2009. Hepatology 62:1723–30.
3. Chalasani N, Younossi Z, Lavine JE, Charlton M, Cusi K, Rinella M, Harrison SA, Brunt EM, Sanyal AJ (2018) The diagnosis and management of nonalcoholic fatty liver disease: Practice guidance from the American Association for the Study of Liver Diseases. The diagnosis and management of nonalcoholic fatty liver disease: Practice guidance from the American Association for the Study of Liver Diseases. Hepatology 67:328–357.
4. Ekstedt M, Hagström H, Nasr P, Fredrikson M, Stål P, Kechagias S, Hultcrantz R (2015) Fibrosis stage is the strongest predictor for disease-specific mortality in NAFLD after up to 33 years of follow-up. Hepatology 61:1547–54.
5. Dulai PS, Singh S, Patel J, Soni M, Prokop LJ, Younossi Z, Sebastiani G, Ekstedt M, Hagstrom H, Nasr P, Stal P, Wong VW, Kechagias S, Hultcrantz R, Loomba R (2017) Increased risk of mortality by fibrosis stage in nonalcoholic fatty liver disease: Systematic review and meta-analysis. Hepatology 65:1557–1565.
6. Pavlides M, Birks J, Fryer E, Delaney D, Sarania N, Banerjee R, Neubauer S, Barnes E, Fleming KA, Wang LM (2017) Interobserver Variability in Histologic Evaluation of Liver Fibrosis Using Categorical and Quantitative Scores. Am J Clin Pathol 147:364–369.
7. Rockey DC, Caldwell SH, Goodman ZD, Nelson RC, Smith AD; American Association for the Study of Liver Diseases (2009) Liver biopsy. Hepatology 49:1017–44.
8. Ganeshan B, Miles KA (2013) Quantifying tumour heterogeneity with CT. Cancer Imaging 13:140–9.
9. Kato H, Kanematsu M, Zhang X, Saio M, Kondo H, Goshima S, Fujita H (2007) Computer-aided diagnosis of hepatic fibrosis: preliminary evaluation of MRI texture analysis using the finite difference method and an artificial neural network. AJR Am J Roentgenol 189:117–22.
10. Daginawala N, Li B, Buch K, Yu H, Tischler B, Qureshi MM, Soto JA, Anderson S (2016) Using texture analyses of contrast enhanced CT to assess hepatic fibrosis. Eur J Radiol 85:511–7.
11. Lubner MG, Malecki K, Kloke J, Ganeshan B, Pickhardt PJ (2017) Texture analysis of the liver at MDCT for assessing hepatic fibrosis. Abdom Radiol (NY) 42:2069–2078.
12. House MJ, Bangma SJ, Thomas M, Gan EK, Ayonrinde OT, Adams LA, Olynyk JK, St Pierre TG (2015) Texture-based classification of liver fibrosis using MRI. J Magn Reson Imaging 41:322–8.
13. Wu Z, Matsui O, Kitao A, Kozaka K, Koda W, Kobayashi S, Ryu Y, Minami T, Sanada J, Gabata T (2015) Hepatitis C related chronic liver cirrhosis: feasibility of texture analysis of MR images for classification of fibrosis stage and necroinflammatory activity grade. PLoS One 10:e0118297.
14. Bahl G, Cruite I, Wolfson T, Gamst AC, Collins JM, Chavez AD, Barakat F, Hassanein T, Sirlin CB (2012) Noninvasive classification of hepatic fibrosis based on texture parameters from double contrast-enhanced magnetic resonance images. J Magn Reson Imaging 36:1154–61.
15. Yokoo T, Wolfson T, Iwaisako K, Peterson MR, Mani H, Goodman Z, Changchien C, Middleton MS, Gamst AC, Mazhar SM, Kono Y, Ho SB, Sirlin CB (2015) Evaluation of Liver Fibrosis Using Texture Analysis on Combined-Contrast-Enhanced Magnetic Resonance Images at 3.0T. Biomed Res Int 2015:387653.
16. Kleiner DE, Brunt EM, Van Natta M, Behling C, Contos MJ, Cummings OW, Ferrell LD, Liu YC, Torbenson MS, Unalp-Arida A, Yeh M, McCullough AJ, Sanyal AJ; Nonalcoholic Steatohepatitis Clinical Research Network (2005) Design and validation of a histological scoring system for nonalcoholic fatty liver disease. Hepatology 41:1313–21.
17. Zhang X, Gao X, Liu BJ, Ma K, Yan W, Liling L, Yuhong H, Fujita H (2015) Effective staging of fibrosis by the selected texture features of liver: Which one is better, CT or MR imaging? Comput Med Imaging Graph 46 Pt 2:227–36.
18. Davnall F, Yip CS, Ljungqvist G, Selmi M, Ng F, Sanghera B, Ganeshan B, Miles KA, Cook GJ, Goh V (2012) Assessment of tumor heterogeneity: an emerging imaging tool for clinical practice? Insights Imaging 3:573–89.
19. Ganeshan B, Miles KA, Young RC, Chatwin CR (2007) Hepatic entropy and uniformity: additional parameters that can potentially increase the effectiveness of contrast enhancement during abdominal CT. Clin Radiol 62:761–8.
20. Miles KA, Ganeshan B, Hayball MP (2013) CT texture analysis using the filtration-histogram method: what do the measurements mean? Cancer Imaging 13:400–6.
21. Lubner MG, Smith AD, Sandrasegaran K, Sahani DV, Pickhardt PJ (2017) CT Texture Analysis: Definitions, Applications, Biologic Correlates, and Challenges. Radiographics 37:1483–1503.
22. Naganawa S, Enooku K, Tateishi R, Akai H, Yasaka K, Shibahara J, Ushiku T, Abe O, Ohtomo K, Kiryu S (2018) Imaging prediction of nonalcoholic steatohepatitis using computed tomography texture analysis. Eur Radiol. 28:3050–3058.
23. Angulo P, Kleiner DE, Dam-Larsen S, Adams LA, Bjornsson ES, Charatcharoenwitthaya P, Mills PR, Keach JC, Lafferty HD, Stahler A, Haflidadottir S, Bendtsen F (2015) Liver Fibrosis, but No Other Histologic Features, Is Associated With Long-term Outcomes of Patients With Nonalcoholic Fatty Liver Disease. Gastroenterology 149:389–97.e10.
24. Horowitz JM, Venkatesh SK, Ehman RL, Jhaveri K, Kamath P, Ohliger MA, Samir AE, Silva AC, Taouli B, Torbenson MS, Wells ML, Yeh B, Miller FH (2017) Evaluation of hepatic fibrosis: a review from the society of abdominal radiology disease focus panel. Abdom Radiol (NY) 42:2037–2053.

25. Wang QB, Zhu H, Liu HL, Zhang B (2012) Performance of magnetic resonance elastography and diffusion-weighted imaging for the staging of hepatic fibrosis: A meta-analysis. Hepatology. 56:239–47.
26. Singh S, Venkatesh SK, Loomba R, Wang Z, Sirlin C, Chen J, Yin M, Miller FH, Low RN, Hassanein T, Godfrey EM, Asbach P, Murad MH, Lomas DJ, Talwalkar JA, Ehman R (2016) Magnetic resonance elastography for staging liver fibrosis in non-alcoholic fatty liver disease: a diagnostic accuracy systematic review and individual participant data pooled analysis. Eur Radiol. 26:1431–40.
27. Tang A, Cloutier G, Szeverenyi NM, Sirlin CB (2015) Ultrasound Elastography and MR Elastography for Assessing Liver Fibrosis: Part 2, Diagnostic Performance, Confounders, and Future Directions. AJR Am J Roentgenol. 205:33–40.
28. Berenguer R, Pastor-Juan MDR, Canales-Vázquez J, Castro-García M, Villas MV, Mansilla Legorburo F, Sabater S (2018) Radiomics of CT Features May Be Nonreproducible and Redundant: Influence of CT Acquisition Parameters. Radiology 288:407–415.
29. Petitclerc L, Gilbert G, Nguyen BN, Tang A (2017) Liver Fibrosis Quantification by Magnetic Resonance Imaging. Top Magn Reson Imaging 26:229–241.
30. Petitclerc L, Sebastiani G, Gilbert G, Cloutier G, Tang A (2017) Liver fibrosis: Review of current imaging and MRI quantification techniques. J Magn Reson Imaging 45:1276–1295.
31. Perrin T, Midya A, Yamashita R, Chakraborty J, Saidon T, Jarnagin WR, Gonen M, Simpson AL, Do RKG (2018) Short-term reproducibility of radiomic features in liver parenchyma and liver malignancies on contrast-enhanced CT imaging. Abdom Radiol (NY) https://doi.org/10.1007/s00261-018-1600-6.
32. Dercle L, Ammari S, Bateson M, Durand PB, Haspinger E, Massard C, Jaudet C, Varga A, Deutsch E, Soria JC, Ferté C (2017) Limits of radiomic-based entropy as a surrogate of tumor heterogeneity: ROI-area, acquisition protocol and tissue site exert substantial influence. Sci Rep 7:7952.
33. Beckers RCJ, Beets-Tan RGH, Schnerr RS, Maas M, da Costa Andrade LA, Beets GL, Dejong CH, Houwers JB, Lambregts DMJ (2017) Whole-volume vs. segmental CT texture analysis of the liver to assess metachronous colorectal liver metastases. Abdom Radiol (NY) 42:2639–2645.
34. Ng F, Kozarski R, Ganeshan B, Goh V (2013) Assessment of tumor heterogeneity by CT texture analysis: can the largest cross-sectional area be used as an alternative to whole tumor analysis? Eur J Radiol. 82:342–8.